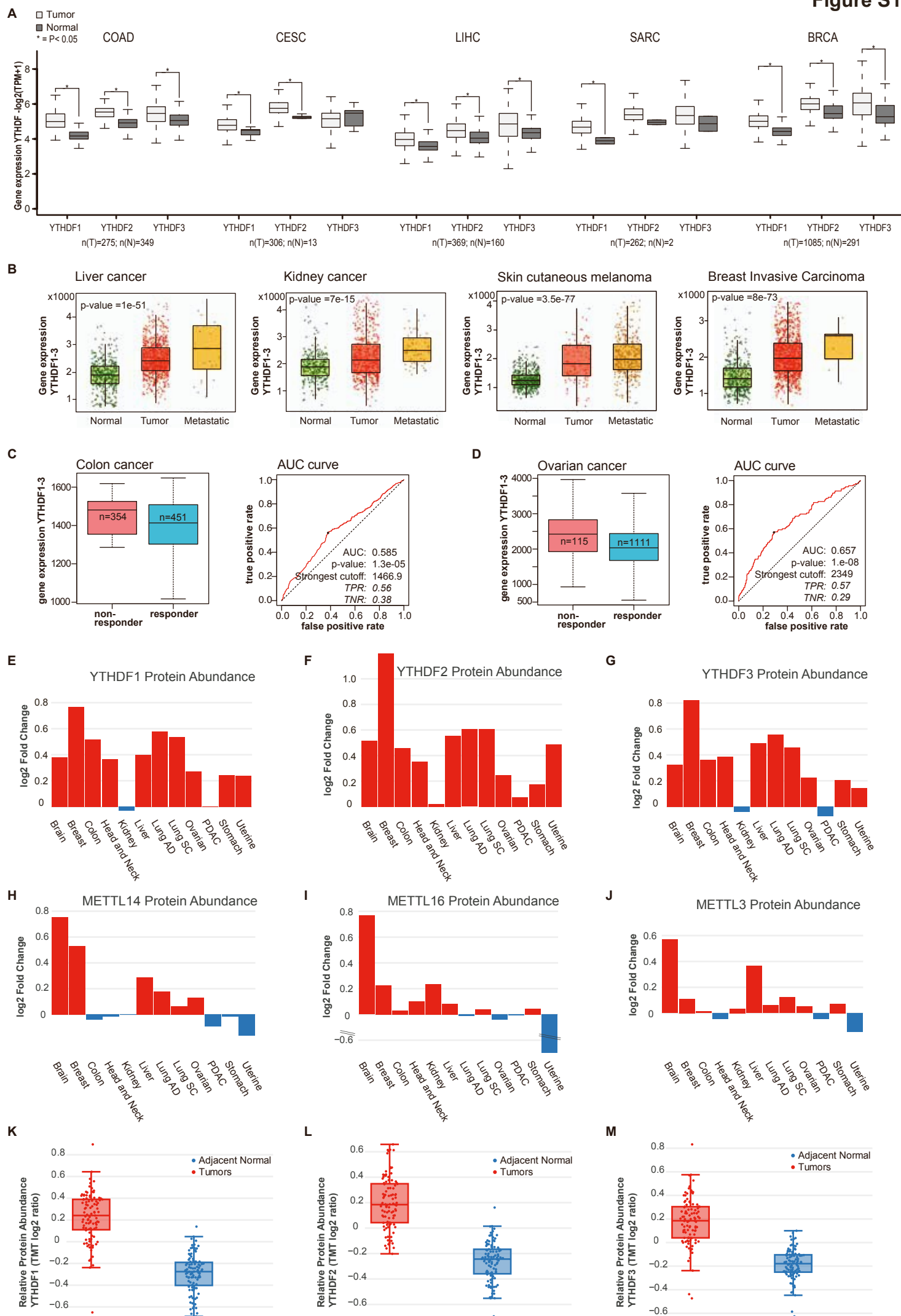


**Supplemental information**

**YTHDF proteins and m<sup>6</sup>A-RNA clients undergo  
autophagic turnover during contact inhibition**

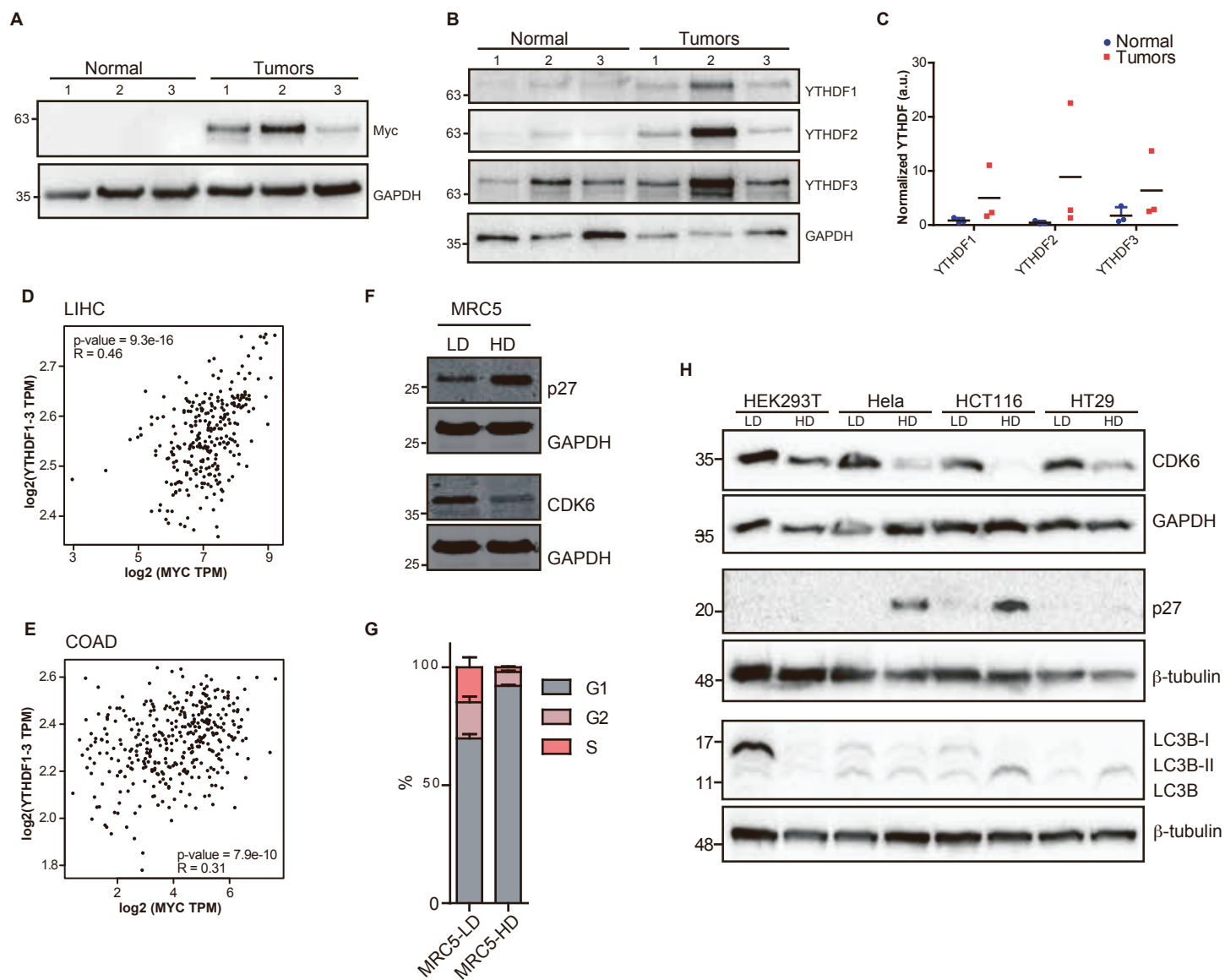
**Hung Ho-Xuan, Astrid Bruckmann, Lautaro Natali, Cristian Prieto-Garcia, Jan F.M. Stuke, Lorene Brunello, Alexandre Vicente, Alexander Pfab, Hagen Wesseling, Sara Cano-Franco, Anshu Khatri, Simone Larivera, Pablo Sanz-Martinez, Benjamin de la Cruz-Thea, Anne-Claire Jacomin, Jan Prochazka, Regina Feederle, Volker Dötsch, Radislav Sedlacek, Gerhard Hummer, Stefanie Kaiser, Ivan Dikic, Melina M. Musri, Gunter Meister, and Alexandra Stolz**

Figure S1



**Figure S1: Gene expression signature of YTHDF protein.** **A)** mRNA expression of YTHDF1, YTHDF2 and YTHDF3 genes (YTHDF1/2/3) in tumor and normal non-transformed tissue for different indicated cancer entities. Gene expression is presented as  $\log_2(\text{TPM}+1)$ , where TPM is transcripts per million. Gepia2 software is described previously (\* $p < 0.05$ ) (see STAR methods). **B)** Gene expression of YTHDF signature (mean gene expression of YTHDF1-3) in normal, tumor, and metastatic samples of Liver cancer, Kidney cancer, Skin cutaneous Melanoma, and Breast Invasive Carcinoma. Data, visualization, and p-value calculation were performed by website [tnmplot.com](http://tnmplot.com) (see STAR methods). The p-value was obtained using Kruskal-Wallis test. **C,D)** Gene expression and ROC (Receiver operating characteristic) curves with AUC calculation (Area under the curve) of YTHDF signature (based on mean gene expression of YTHDF1-3) in non-responder and responder. Data, visualization, and p-value calculation were performed by website [rocplot.com](http://rocplot.com) (see STAR methods). TPR = true positive rate; TNR = true negative rate. **E-J)** Protein expression level of indicated proteins across different tumors compared to their corresponding normal tissues. Data and visualization from the publicly available NIH database cProSite - Cancer Proteogenomic Data Analysis Site (<https://cprosite.ccr.cancer.gov/>). **K-M)** Relative protein abundance of YTHDF1, YTHDF2, and YTHDF3 in colon cancer tumors and adjacent healthy tissues. Data and visualization from the publicly available NIH database cProSite - Cancer Proteogenomic Data Analysis Site (<https://cprosite.ccr.cancer.gov/>). Unpaired p-value:  $< 0.0001$ .

**Figure S2**



**Figure S2: Correlation between expression of YTHDF protein with cMYC and expression of p27 and CDK6 in cells at low density (LD) and high density (HD).** **A-B)** Western blot analysis of cMYC (**A**) and YTHDF (**B**) protein levels in primary liver tumors (Myc OE; TP53Δ) and surrounding healthy tissue from MycOE; TP53Δ liver cancer mouse model (see Star methods). n=3 mice. **C)** Quantification of B. **D, E)** correlation between MYC and YTHDF genes (1,2 and 3 together) in human Liver Hepatocellular Carcinoma (LIHC) (D) and Colon Adenocarcinoma (COAD) tumors (E). **F)** Western blot analysis of MRC5 cells harvested at LD and HD. p27 and CDK6 served as markers for cell cycle regulation. **G)** Cell cycle analysis of MRC5 cells at LD and HD. Data represents the average of three biological replicates. Error bars = SD. **H)** Western blot analysis of p27, CDK6, and LC3B from non-contact-inhibited cells (HEK293T, Hela, HCT116, HT29) cells harvested at LD and HD. GAPDH and beta-tubulin served as loading control while p27, and CDK6 served as markers for cell cycle regulation.

Figure S3

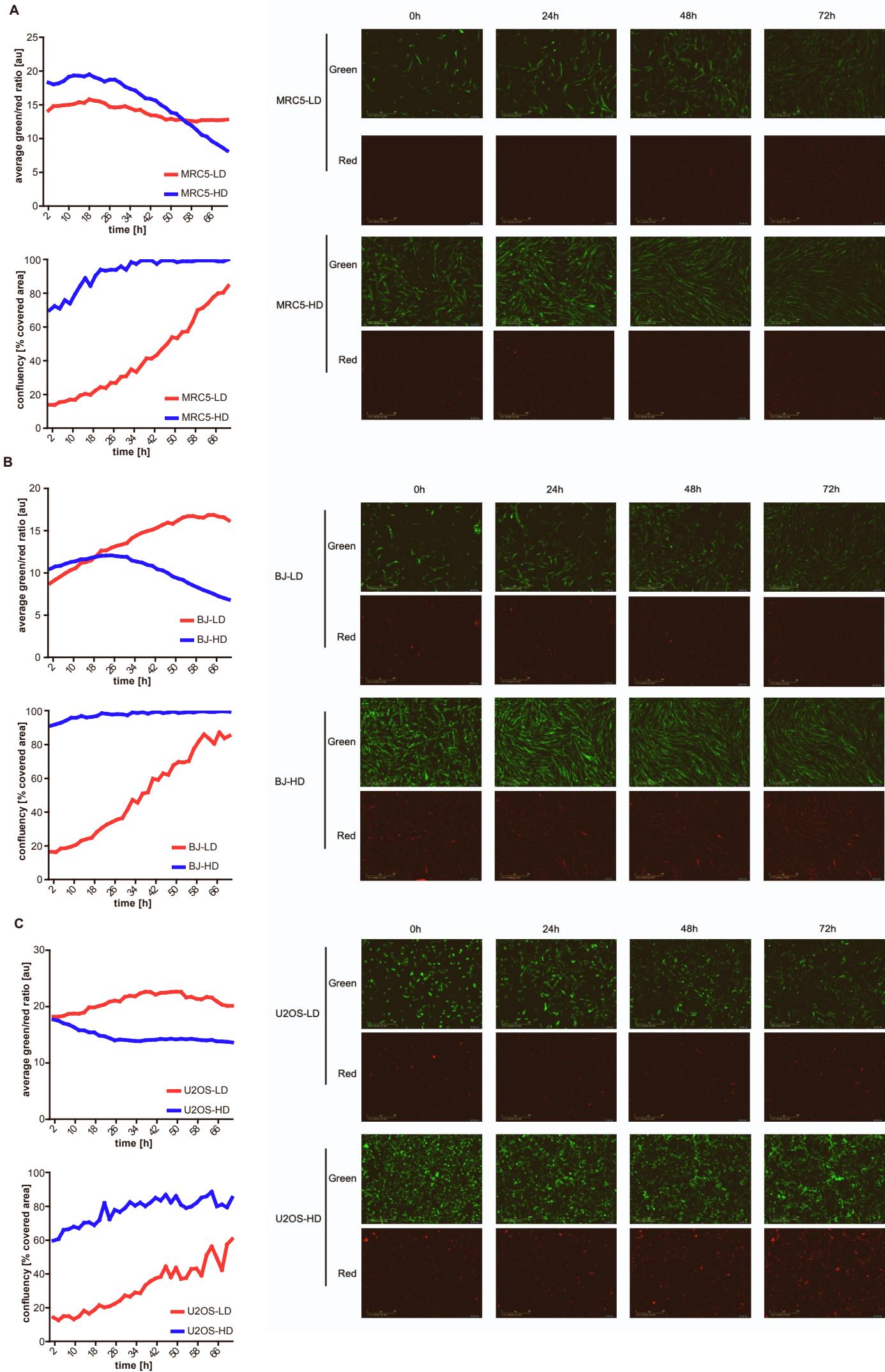


**Figure S3: Autophagy flux in MRC5 and U2OS expressing the reporter EGFP-LC3-RFP-LC3 $\Delta$ G.**  
**A-C)** Autophagy flux (top left panel, low ratio=high flux), confluence (bottom left panel), and representative images (right panels) of MRC5 (**A**), BJ (**B**), and U2OS (**C**) cells stably expressing the autophagy flux reporter EGFP-LC3-RFP-LC3 $\Delta$ G and seeded at LD and HD.



Figure S4

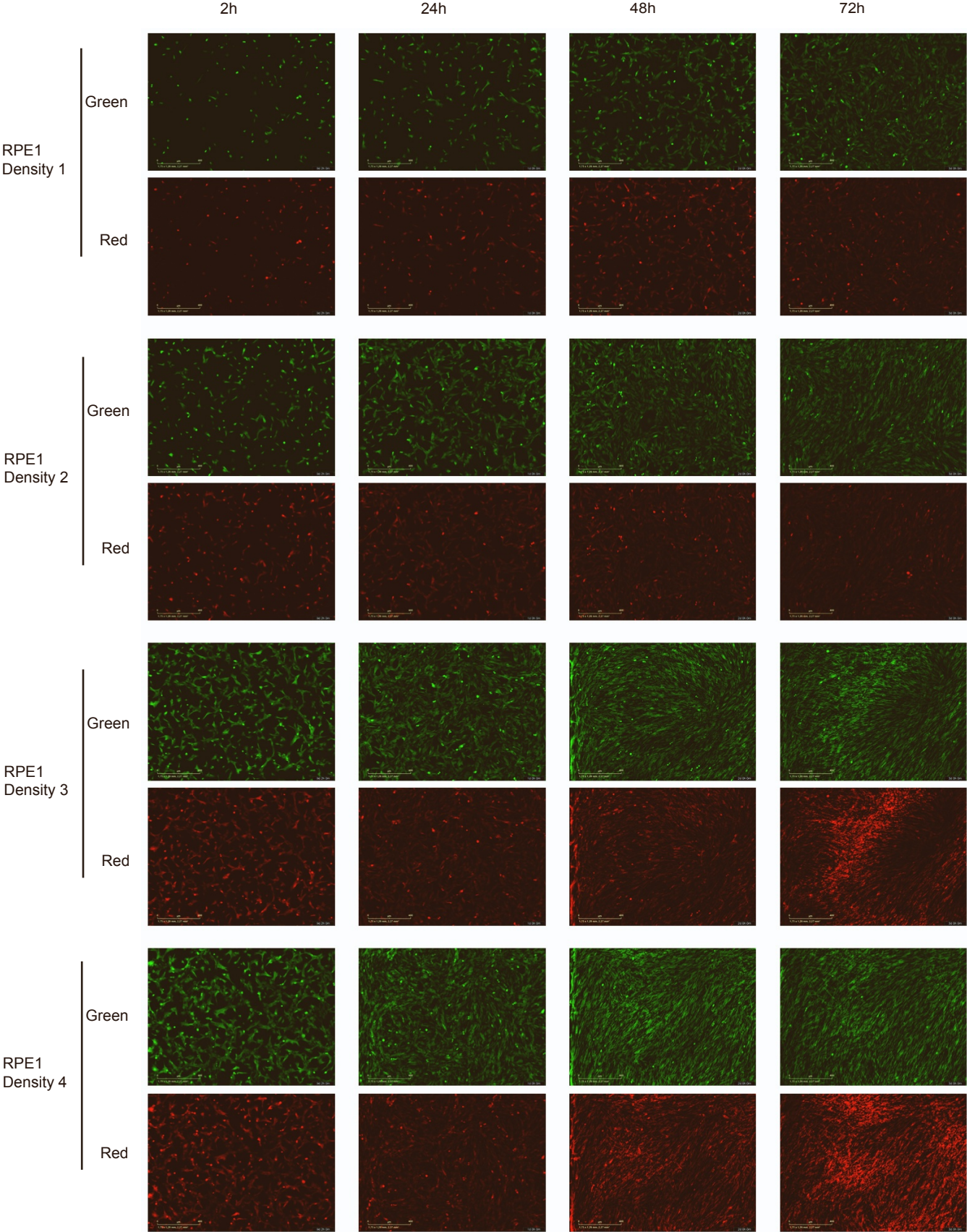




**Figure S4: Autophagy flux in RPE1 cells expressing the reporter EGFP-LC3-RFP-LC3 $\Delta$ G.**  
Representative images of RPE1 cells expressing autophagy flux reporter EGFP-LC3-RFP-LC3 $\Delta$ G seeded at four different densities at different time points (0h, 24h, 48h, and 72h).

Figure S5

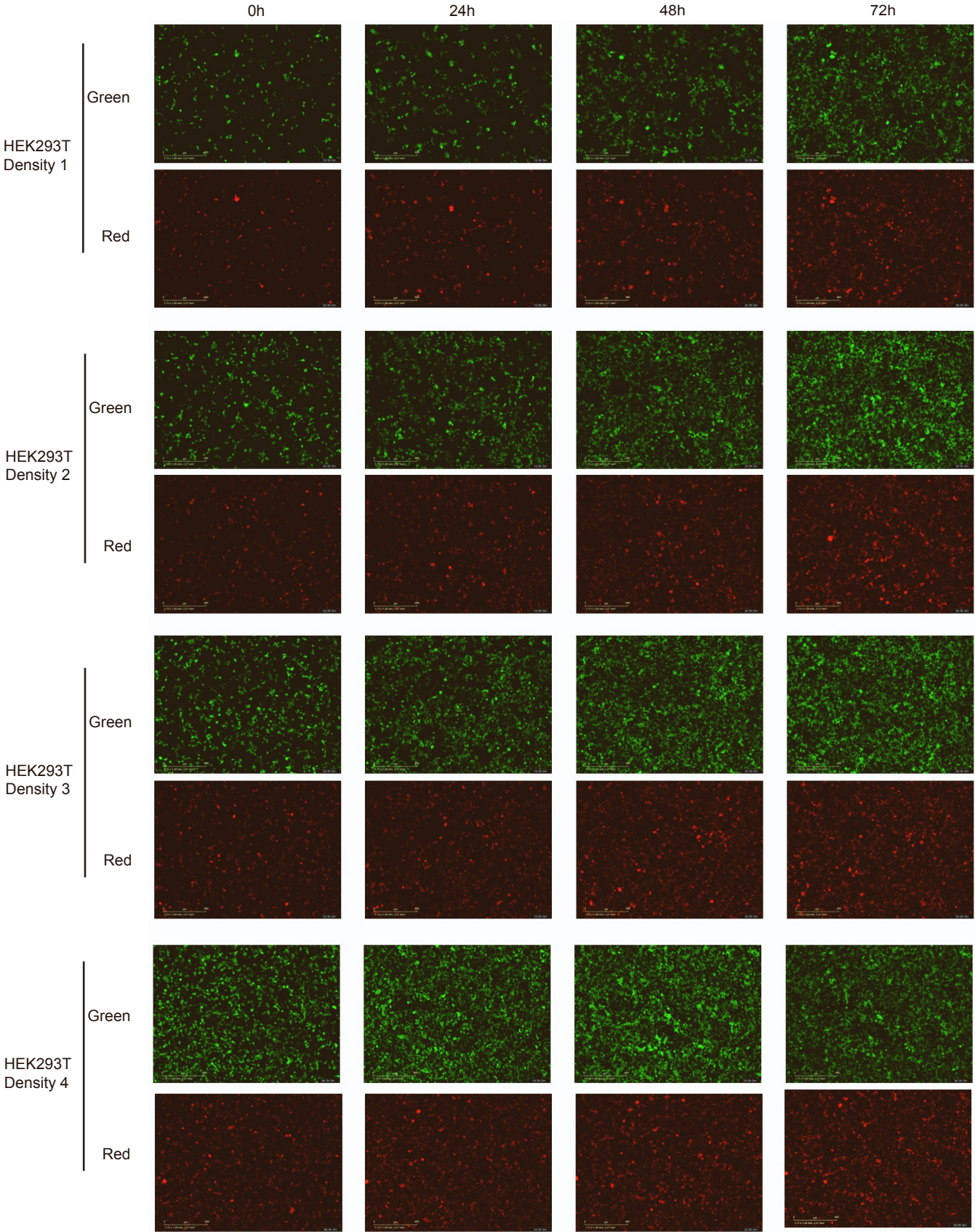


**Figure S5: Autophagy flux in HEK293T cells expressing the reporter EGFP-LC3-RFP-LC3 $\Delta$ G.**

Representative images of HEK293T cells expressing the autophagy flux reporter EGFP-LC3-RFP-LC3 $\Delta$ G seeded at four different densities at different time points (0h, 24h, 48h, and 72h).

**Figure S6**

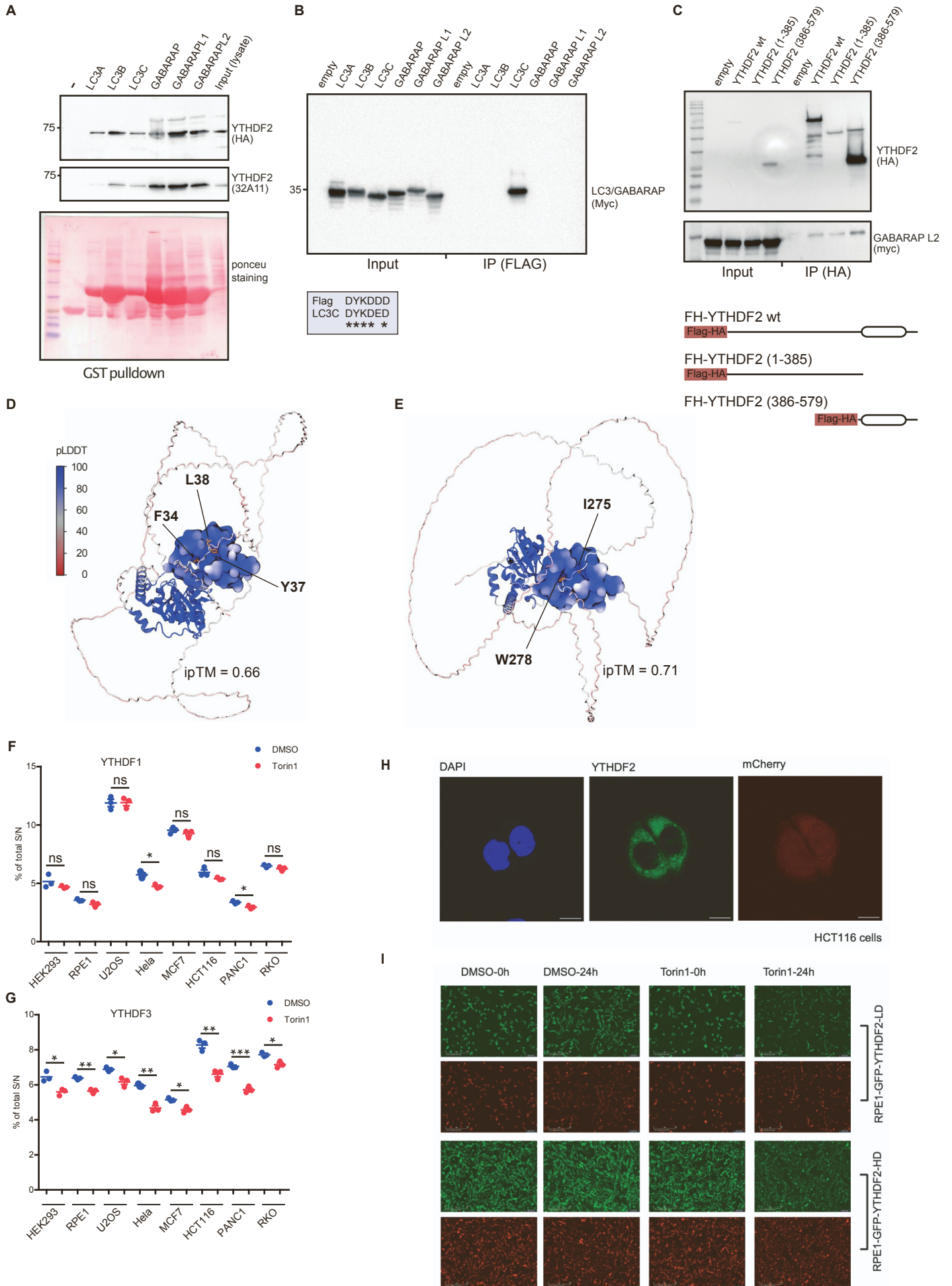
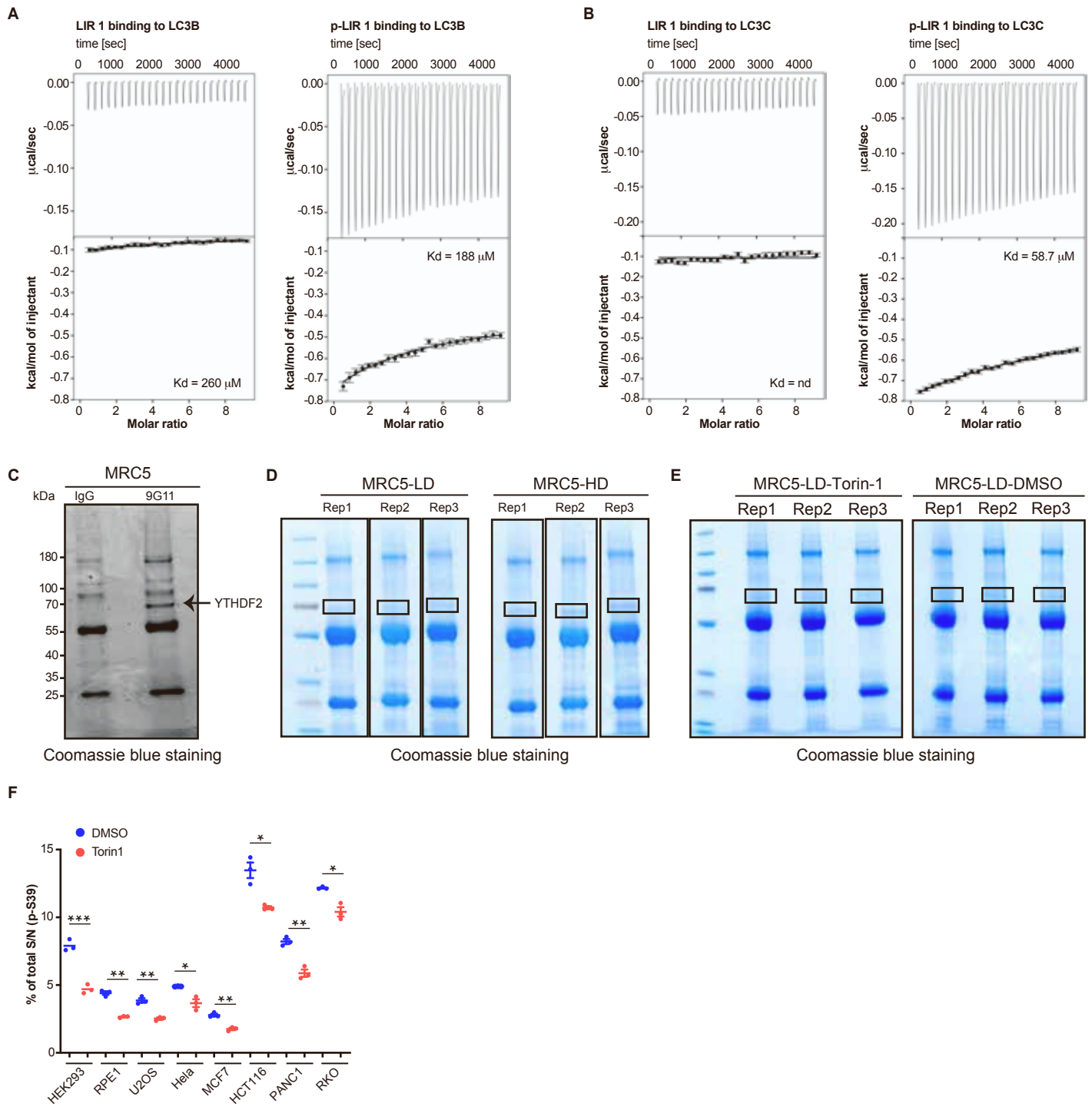




**Figure S6: Binding of YTHDF2 with GABARAP L2** **A)** GST pull-down assay testing the binding of GST-tagged LC3/GABARAP with YTHDF2. **B)** Immunoprecipitation of Myc-tagged LC3/GABARAPs with only anti-Flag beads. Lower panel highlights the sequence similarity between the FLAG tag and LC3C. **C)** Lower panel: Schematic overview of YTHDF2 wt domain and the truncated versions: N terminal (YTHDF2 1-385) and C terminal (386-579) with Flag/HA tag at the N terminal. Upper panel: Co-immunoprecipitation analysis in transiently transfected HEK293T cells co-expressing Myc-tagged GABARAP L2 proteins and Flag-HA-tagged YTHDF2 wt and two truncated versions using anti-HA beads. **D-E)** AlphaFold3 predictions of GABARAP L2 and YTHDF2 suggest binding of YTHDF2 residues 34-FEPYL-37 (left) and 275-IGTW-278 (right) to GABARAP L2 in different models. YTHDF2 is shown in cartoon and GABARAP L2 in surface representation. Both are colored by pLDDT score. Residues of YTHDF2 engaging hydrophobic pockets (HPs) 1 and 2 are highlighted as orange licorice. **F-G)** Relative protein expression level of YTHDF1 (F) and YTHDF3 (G) proteins in different cell lines upon treatment with 150 nM Torin1. Data was extracted and reanalyzed from the dataset published previously [S1]. \*p < 0.05, \*\*p < 0.01, \*\*\*p < 0.001, ns (not significant). **H)** Immunofluorescent images of HCT116 cells expressing EGFP-YTHDF2 and mCherry as an internal control. **I)** Representative images of RPE1 cells expressing the autophagy flux reporter EGFP-YTHDF2-p2A-mCherry seeded at LD and HD and treated with 0.1% DMSO and 250nM Torin1 at time point 0 and 24 h after treatment.

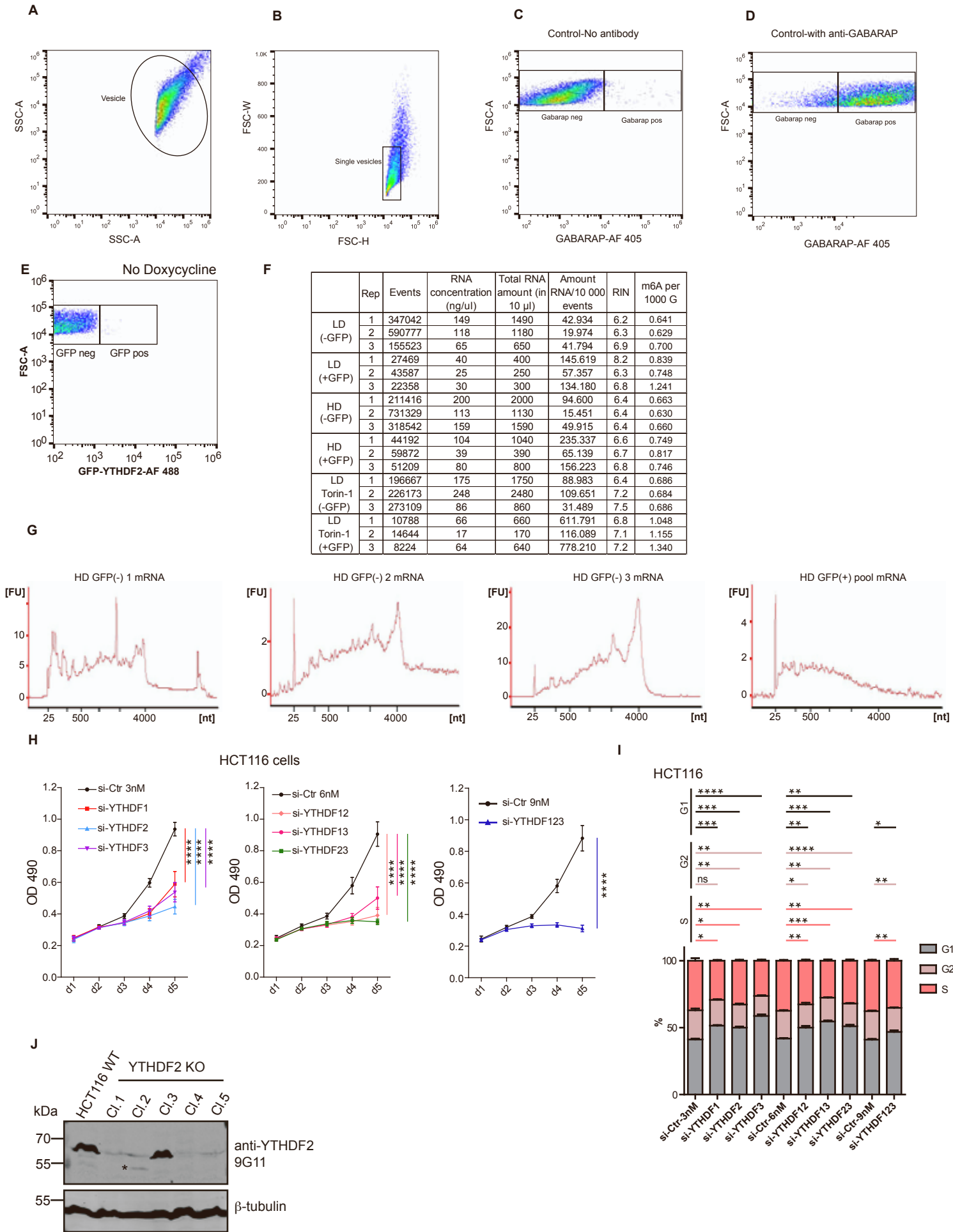


Figure S7



**Figure S7: Interaction of LIR1 with LC3B and LC3C, and Coomassie staining of immunoprecipitation for identification of S39 phosphorylation. A-B)** Interaction profile of LIR1 titrated to the members of mATG8 family (A) LC3B, (B) LC3C. Every measurement was done at 25 °C by titrating 700  $\mu$ M of peptide to 14  $\mu$ M of ATG8. The top panel of each figure shows the raw titration profile and the bottom panel displays the integrated heat of each titration event. The best fit of a single-site binding model is shown as a solid black line, generated by GUSI software. The resulting equilibrium dissociation constant ( $K_d$ ) is mentioned at the bottom of every plot. **C)** Coomassie blue staining of the immunoprecipitation from MRC5 cells using IgG and anti-YTHDF2 clone 9G11. A band marked by the arrow represents YTHDF2, which is further verified by mass spectrometry. **D-E)** Coomassie blue staining of the immunoprecipitation from MRC5 cells seeded at low (LD) and high density (HD) (D) or seeded at LD and treated with 0.1% DMSO or 250nM Torin-1 (E) after immunoprecipitation with anti-YTHDF2 clone 9G11. A black box indicates the band of YTHDF2 that was sliced for targeted proteomics quantification. **F)** Relative protein expression level of S39 phosphorylation on YTHDF2 in different cell lines upon treatment with 150 nM Torin1. Data was extracted and reanalyzed from the dataset published previously [S1]. Data represent mean with standard deviation (SD). Statistics analysis was calculated using Student's *t*-test (\* $p < 0.05$ , \*\* $p < 0.01$ ) by GraphPad Prism 10.

Figure S8



**Figure S8: Establishment of FACS-based autophagosome isolation and characterization of YTHDF depletion. A-E)** Scatterplot from FACS analysis showing the steps of autophagosome isolation. Panels show selection of vesicle population (A), single vesicle population (B), selection of autophagosomes without antibody control (C) with anti-GABARAP (D), and gating of GFP-negative and GFP-positive autophagosomes without doxycycline treatment (E). **F)** Table summarizing information related to RNA content of autophagosomes isolated from GFP-negative and GFP-positive autophagosomes of RPE1 cells expressing EGFP-YTHDF2-p2A-mCherry cultured in LD, HD and LD treated with 250nM of Torin1. **G)** Bioanalyzer electrophoresis of mRNA isolated from GFP-negative and GFP-positive autophagosomes of RPE1 cells expressing EGFP-YTHDF2-p2A-mCherry cultured in HD. **H)** HCT116 cells were seeded in 96-well plates, and XTT assays of the effect of YTHDF protein knockdown on cell proliferation were performed over five days. n=3; error bars=SD Statistics analysis was calculated using two-way ANOVA (\*\*\*\*p < 0.0001) by GraphPad Prism 10. **I)** Cell cycle analysis of HCT116 upon knockdown of YTHDF proteins two days after transfection. n=3; error bars=SD. Statistics analysis was calculated using Student's *t*-test by GraphPad Prism 10. . \*p < 0.05, \*\*p < 0.01, \*\*\*p < 0.001, \*\*\*\*p < 0.0001, ns (not significant). **J)** Western blot of different CRISPR/Cas9-mediated knockout clones of YTHDF2 in HCT116.Luc cell lines

#### Supplemental reference list

[S1]. Li, J., Van Vranken, J.G., Pontano Vaite, L., Schweppe, D.K., Huttlin, E.L., Etienne, C., Nandhikonda, P., Viner, R., Robitaille, A.M., Thompson, A.H., et al. (2020). TMTpro reagents: a set of isobaric labeling mass tags enables simultaneous proteome-wide measurements across 16 samples. *Nat. Methods* 17, 399–404. 10.1038/s41592-020-0781-4.